jove

High Throughput Image-Based Phenotyping for Determining Morphological and Physiological Responses to Single and Combined Stresses in Potato

Lamis Osama Anwar Abdelhakim[1], **Barbora Pleskačová**[1], **Natalia Yaneth Rodriguez-Granados**[2], **Rashmi Sasidharan**[2], **Lucia Sandra Perez-Borroto**[3], **Sophia Sonnewald**[4], **Kristina Gruden**[5], **Ute C. Vothknecht**[6], **Markus Teige**[7], **Klára Panzarová**[1]

[1] PSI (Photon Systems Instruments), spol. s r.o. Drasov [2] Plant Stress Resilience, Institute of Environmental Biology, Utrecht University [3] Plant Breeding, Wageningen University and Research [4] Department of Biology, Biochemistry, Friedrich-Alexander Universität Erlangen-Nürnberg [5] Department of Biotechnology and Systems Biology, National Institute of Biology [6] Plant Cell Biology, Institute of Cellular and Molecular Botany, University of Bonn [7] Department of Functional & Evolutionary Ecology, University of Vienna

Corresponding Author

Lamis Osama Anwar Abdelhakim
abdelhakim@psi.cz

Citation

Abdelhakim, L.O.A., Pleskačová, B., Rodriguez-Granados, N.Y., Sasidharan, R., Perez-Borroto, L.S., Sonnewald, S., Gruden, K., Vothknecht, U.C., Teige, M., Panzarová, K. High Throughput Image-Based Phenotyping for Determining Morphological and Physiological Responses to Single and Combined Stresses in Potato. *J. Vis. Exp.* (208), e66255, doi:10.3791/66255 (2024).

Date Published

June 7, 2024

DOI

10.3791/66255

URL

jove.com/video/66255

Abstract

High throughput image-based phenotyping is a powerful tool to non-invasively determine the development and performance of plants under specific conditions over time. By using multiple imaging sensors, many traits of interest can be assessed, including plant biomass, photosynthetic efficiency, canopy temperature, and leaf reflectance indices. Plants are frequently exposed to multiple stresses under field conditions where severe heat waves, flooding, and drought events seriously threaten crop productivity. When stresses coincide, resulting effects on plants can be distinct due to synergistic or antagonistic interactions. To elucidate how potato plants respond to single and combined stresses that resemble naturally occurring stress scenarios, five different treatments were imposed on a selected potato cultivar (*Solanum tuberosum* L., cv. Lady Rosetta) at the onset of tuberization, i.e. control, drought, heat, waterlogging, and combinations of heat, drought, and waterlogging stresses. Our analysis shows that waterlogging stress had the most detrimental effect on plant performance, leading to fast and drastic physiological responses related to stomatal closure, including a reduction in the quantum yield and efficiency of photosystem II and an increase in canopy temperature and water index. Under heat and combined stress treatments, the relative growth rate was reduced in the early phase of stress. Under drought and combined stresses, plant volume and photosynthetic performance dropped with an increased temperature and stomata closure in the late phase of stress. The combination of optimized stress treatment under defined environmental conditions together with selected phenotyping protocols allowed to reveal the dynamics of morphological and physiological responses to single and combined stresses. Here, a

useful tool is presented for plant researchers looking to identify plant traits indicative of resilience to several climate change-related stresses.

Introduction

The potential effects of climate change, including the increase in the intensity and frequency of heat waves, flooding, and drought events, have negative impacts on growing crops[1]. It is important to understand the influence of climate change on crop variability and the consequent fluctuations in annual crop production[2]. With increasing population and food demand, maintaining the yield of crop plants is a challenge, thereby, finding climate-resilient crops for breeding is urgently required[3,4]. Potato (*Solanum tuberosum* L.) is one of the essential food crops that contributes to global food security because of its high nutritional value and increased water use efficiency. However, reduction in growth and yield under unfavorable conditions is a main problem, particularly in the susceptible varieties[5,6]. Many studies highlighted the importance of investigating alternative approaches to maintain potato crop productivity, including agricultural practices, finding tolerant genotypes, and understanding the impact of stress on the development and yield[7,8,9], which is also highly demanded by European potato growers (or farmers)[10].

Automated phenotyping platforms, including image-based phenotyping, enable the quantitative analyses of plant structure and function that are essential for selecting relevant traits of interest[11,12]. High throughput phenotyping is an advanced non-invasive technique to determine various morphological and physiological traits of interest in a reproducible and rapid manner [13]. Although phenotype reflects genotypic differences in connection to environmental effects, comparing plants under controlled conditions with stress enables linking the extensive phenotyping information to a specific (stress) condition[14]. Image-based phenotyping is essential in describing phenotypic variability, and it is also capable of screening a set of traits across plant development regardless of the population size[15]. For instance, the measurement of morphological traits, including the shape, size, and color index of leaves using Red-Green-Blue (RGB) imaging sensors, is used to determine plant growth and development. Moreover, measurements of physiological traits, including photosynthetic performance, canopy temperature, and leaf reflectance, are quantified using multiple types of sensors, such as chlorophyll fluorescence, thermal infrared (IR), and hyperspectral imaging[16]. Recent studies in controlled environments showed the potential of using image-based phenotyping in assessing different mechanisms and physiological responses of plants under abiotic stresses such as heat in potato[17], drought in barley[18], rice[19], and combined drought and heat treatments in wheat[20]. Even though studying the responses of plants to multiple stress interactions is complex, the findings reveal new insights in understanding plant mechanisms in coping with rapid change in climate conditions[21].

Plant physiological and morphological responses are directly influenced by abiotic stress conditions (high temperature, water deficit, and flooding), resulting in yield reduction[22]. Even though potatoes have a high water use efficiency compared to other crops, water deficit negatively affects the yield quantity and quality due to the shallow root

architecture[5]. Depending on the intensity and duration of drought level, the leaf area index is reduced, and retardation in canopy growth with inhibition of new leaf formation is pronounced during later stages of stress leading to a reduction in the photosynthetic rate[23]. The threshold level of water is critical with excess water or prolonged drought periods, resulting in a negative effect on plant growth and tuber development due to oxygen limitation, decreased root hydraulic conductivity, and restriction of gas exchange[24,25]. Moreover, potatoes are sensitive to high temperatures where temperatures above optimum levels result in delayed tuber initiation, growth, and assimilation rates[26]. When stresses appear in combination, the biochemical regulations and physiological responses differ from individual stress responses, highlighting the necessity of investigating the plant responses to stress combinations[27]. Combined stresses can result in (even more) severe reductions in plant growth and determinantal effects on reproductive-related traits[28]. The impact of stress combination depends on the dominancy of each stress over the others, leading to enhanced or suppressed plant response (e.g., drought usually leads to stomata closure while stomata are open to allow cooling of leaf surface under heat stress). However, combined stress research is still emerging, and further investigations are required to understand better the complex regulation mediating plant responses under these conditions[29]. Thus, this study aims to highlight and recommend a phenotyping protocol using multiple imaging sensors that can be suitable to assess morpho-physiological responses and understand the underlying mechanisms of potato overall performance under single and combined stress treatments. As hypothesized, combining multiple imaging sensors proved to be a valuable tool to characterize the early and later strategies during plant stress response. Optimizing image-based phenotyping protocol will be an interactive tool for plant researchers and breeders to find traits of interest for abiotic stress tolerance.

Protocol

1. Plant material preparation and growth conditions

1. Transplant *in vitro* Potato (*Solanum tuberosum* L., cv. Lady Rosetta) cuttings from tissue culture into 250 mL pots.
2. Fill the pots with fully saturated Klasmman Substrate 2 and keep them in the growth chamber under low light conditions for 1 week.
3. Adjust the light conditions on the canopy level to 160 $\mu mol \cdot m^{-2} \cdot s^{-1}$ with a combination of 25% white light and 35% infrared using a light meter.
4. Transplant the plants after 10 days of growing the *in vitro* cuttings in soil into 3 L pots (15.5 cm diameter, 20.5 cm height).
5. Fill the 3 L pot with 1850 g of 3:1 Klasmann Substrate 2: Sand.
6. Place the plants in the growth chamber under light conditions of 320 $\mu mol \cdot m^{-2} \cdot s^{-1}$ with a combination of 55% white light and 81% infrared and set it to a long day regime (16 h photoperiod).
7. Set the temperature in the growth chamber to 22 °C/19 °C for day/night and relative humidity (RH) to 55% for the entire experiment.
8. Maintain the pot weight at 60% soil relative water content (SRWC) as the suitable control level to maintain the growth and yield[30,31].

NOTE: Based on previous trials, maintaining volumetric water content above 60% promoted moss growth on the soil surface and elevated the risk of plant diseases. Additionally, the presence of moss could generate misleading positive signals from chlorophyll fluorescence imaging, which is challenging to filter out. Use the following equation: SRWC% = (FW-DW)/(TW-DW) × 100, where FW is the soil fresh weight, TW is the turgor weight, and DW is the dry weight[32].

1. Select the soil samples (100 g) from three different Klasmman Substrate 2 mixture bags as replicates and weigh the fresh weight of the soil.
2. Saturate the soil with water until pots hold water without dripping and weigh soil turgor weight.
3. Place the sample in the oven at 80 °C for 3 days until soil samples are dry completely and weigh the soil dry weight[33].

9. Place the blue mats on the pot surface to reduce evaporation.
   NOTE: Blue color is necessary to subtract the soil background from plant pixels in the image segmentation.
10. Select ten biological replicates per treatment.
11. Randomize the pots during irrigation (in total, 50 pots).
12. Add the blue holders to support the plants and avoid mechanical damage when placing them in the phenotyping system.

2. Stress application

1. At the early tuberization stage (28 days after transplanting the *in vitro* cuttings), divide the plants into five treatment groups and phenotype ten plants per treatment (**Figure 1**).
2. Induce the single and combined stress to a level that is not detrimental as follows:
   1. In the growth chamber, keep the plants under control, drought, and waterlogging treatments at 22 °C/19 °C day/night (step 1.7), with different percentages of SRWC:
      Control (C) with 60% SRWC for the entire experiment.
      Drought (D) with 20% SRWC gradually for 7 days, followed by 1 day of recovery.
      Waterlogging (W) with 160% SRWC for 5 days, followed by 10 days of recovery.
   2. To maintain the water level above the soil surface in the waterlogging treatment, insert a plastic bag into the empty pot and then place the main pot with soil into the prepared second pot.
   3. Place the plants in a growth capsule at 30/28 °C day/night and 55% RH for heat treatments. Impose single and combined heat stresses as follows:
      1. For Heat (H), maintain the temperature 30-28 °C with 60% of SRWC for 15 days.
      2. For Heat + Drought + Waterlogging (HDW) triple stress, expose the plants to heat treatment at 30 °C/28 °C day/night temperature for the first 7 days (keeping 60% SRWC), followed by drought + heat combined treatment for the other 7 days (20% SRWC and 30 °C/28 °C) and finally expose the plants to waterlogging stress for 1 day. For the latter, place the plants back in the growth chamber (see step 1.7 for conditions) and induce waterlogging to 160% SRWC for 1 day.

NOTE: The selected durations of the induced stresses were based on a pilot experiment that showed stress effects without detrimental impacts with 100% survival of the treated plants. In the growth chamber environment, the variation of environmental conditions was in the range ± 0.2 °C for temperature and ± 3% for humidity.

3. Plant preparation for phenotyping

1. After lights are turned on at 6:00 am in the growth chambers, allow plants to acclimatize under the constant growth light conditions (320 µmol·m^{-2}·s^{-1}) for at least 2-3 h before the phenotyping protocol initiation. This ensures that photosynthesis and stomatal regulation are in a steady state[34].
2. Before the measurement, transfer the plants from their cultivation location into the growth buffer area of the phenotyping system used for manual loading of plants into the system while automated scoring is in standby mode and positioned within the greenhouse (**Supplementary Figure 1, Supplementary Figure 2**, and **Supplementary Figure 3**).
   NOTE: Plants were kept in the growth buffer area during the phenotyping period lasting 3.5 h. In the greenhouse, the variation of environmental conditions was in the range of ± 2 °C for temperature, ± 5% for humidity, and 20% fluctuation in the light intensity. Thus, consider that the measurements should start immediately and be short, avoiding the influence of greenhouse conditions on plants.
3. In the phenotyping platform, place the pots in the disks that automatically move on a conveyor belt in given intervals to the imaging sensor according to the measurement protocols specified in section 4.
4. Label each plant/tray with a unique ID to ensure the measured data is assigned to the correct plant throughout the experiment.

4. Phenotyping protocol

1. Optimize the phenotyping protocol using multiple imaging sensors (chlorophyll fluorescence, thermal IR, RGB, and hyperspectral imaging), thereby allowing simultaneous measurement of both the physiological and morphological parameters of plants (**Figure 2**).
   NOTE: Since plant responses reflect the environmental conditions and diurnal effects, it is important to consider randomization of the pots and performing phenotyping within the same period of the day.
2. In the phenotyping platform, ensure that the plants enter the system through an adaptation tunnel (**Figure 2A**) where the height of the plant is captured first, and then the height of each sensor is adjusted based on fixed working distance.
3. Conduct the measurements in two rounds as justified in the measuring protocol using the software.
   1. In the first round, comprise the measurements of physiological responses quantified as "fast reactions" using chlorophyll fluorescence and thermal imaging.
   2. Start by measuring the physiological parameters under heat stress treatments and then the rest of the treatments.
   3. In the second round, proceed with other measurements for assessing slower responses,

including structural RGB and hyperspectral imaging, followed by weight assessment and watering.

4. During the weighing and watering step, define the reference weight for each plant to enable automated watering and weighing to the given treatment.
    1. Ensure the total reference weight includes the weight of the disk, insert located on the conveyor belt, supporting blue holder, blue mat, pot, soil, and plant biomass in the defined protocol.
    2. For accurate measurement of evapotranspiration during the weighing and watering step, prepare empty pots as a reference. In addition, prepare additional pots to correct for plant biomass weight.
5. To measure 50 plants, the whole phenotyping protocol duration takes 215 min (85 min in the 1st round and 130 min in the 2nd round).
6. Phenotype daily all plants under control conditions (1 day before the treatment) and then induce the stress treatments to monitor the dynamic responses and assess the early and late phases of the induced stress.

5. Adjusting settings for each imaging sensor

1. Kinetic chlorophyll fluorescence imaging

    NOTE: Kinetic chlorophyll fluorescence is used to investigate the photosynthetic capacity of plants in response to different environmental conditions, including abiotic stresses, and to provide valuable information about the quantum efficiency of photochemistry and heat dissipation (non-photochemical process).
    1. Conduct chlorophyll fluorescence measurement on light-adapted plants using a short light protocol to discriminate responses of plants under different treatments.
    2. Acclimate[35] the plants for 5 min under the light in the adaptation tunnel equipped with cool-white LEDs (6500 K) at 500 µmol·m^{-2}·s^{-1}.

        NOTE: Chlorophyll fluorescence imaging is the first measurement after the light adaptation used to monitor changes in the photosynthetic capacities of plants.
    3. Select and optimize the pre-defined protocol according to the plant size and required light intensities.
    4. Optimize the measurement settings, including camera and light intensity settings to ensure the acquisition of a strong signal with an optimal signal-to-noise ratio.
        1. Adjust camera settings such as shutter (exposure time, duration of measuring flashes) and sensitivity (electrical gain of the camera). Use the shutter at 2 ms and sensitivity at 12%.

            NOTE: These values being adjusted based on the leaf size and shape and the defined distance between the top of the canopy and the imaging sensor.
        2. Adjust the actinic light intensity at 500 µmol·m^{-2}·s^{-1} and set the saturation pulse at 3200 µmol·m^{-2}·s^{-1}, which is at least 6-7 times higher than the actinic light.
    5. To measure parameters in light steady-state (Lss) (described below) light-adapt plants for 5 min before the measurements in the light adaptation tunnel.

6. To estimate the steady-state photosystem II (PSII) quantum yield of light-adapted plants, select the short light protocol (**Figure 3**) and set the protocol as follows.

   NOTE: The protocol duration was 10 s per plant.

   1. Start the measurement by turning on the cool-white actinic light at 500 $\mu mol \cdot m^{-2} \cdot s^{-1}$ for 3 s to measure the steady-state fluorescence in light (F_t_Lss aka. F_t')

   2. Apply saturation pulse at 3200 $\mu mol \cdot m^{-2} \cdot s^{-1}$ for 800 ms to measure the steady-state maximum fluorescence in light (F_m_Lss aka. F_m')

   3. Turn off the actinic light, then turn on the far-red light (735 nm) to enable PSII to relax in the dark for 800 ms and measure the steady-state minimum fluorescence in light (F_o_Lss aka. F_o').

7. To calculate the relative parameters, use data analyzer software that subtracts the background and extracts the relevant parameters.

   NOTE: Parameters extracted from the used protocol are: maximum efficiency of PSII photochemistry of light-adapted sample in light steady-state determined as F_v/F_m_Lss aka. F_v'/F_m', photosystem II quantum yield or operating efficiency of photosystem II in light steady-state defined as QY_Lss aka. $\varphi_{PSII} = F_q'/F_m'$, and the fraction of open reaction centers in PSII (oxidized QA) is determined as qL_Lss = $(F_q'/F_v') \times (F_0'/F_t')$.

2. Thermal Infrared (IR) imaging

   NOTE: Thermal IR imaging is used for non-invasive measurement of actual canopy temperature, thereby determining the different stomatal regulations. In the thermal IR imaging unit, a thermal camera is mounted laterally on the robotic arm to measure the canopy temperature from the side view.

   1. To increase the contrast of the background temperature over the temperature of the imaged object during the image processing, use an automatically controlled heated wall on the opposite side of the thermal camera to increase the contrast. Regulate the wall temperature at 8 °C above the air temperature in the imaging unit.

      NOTE: The thermal images were acquired in darkness using line scan mode[35].

   2. After image acquisition, generate a plant mask based on RGB side-view data and employ it to co-register with thermal data in the image analysis. This ensures precise identification of the scanned object while eliminating background interference such as plant holder.

   3. To prevent the influence of fluctuating environmental conditions throughout the entire experiment, calculate the parameter temperature difference (delta T or ΔT).

      NOTE: Delta T (ΔT) is defined as the difference between the measured temperature of the leaf surface (the average of all pixels from the entire detected surface of the plant) and the ambient air temperature inside the imaging box.

3. RGB imaging

   NOTE: RGB imaging is based on visual inertial system (VIS) cameras that detect light in the visible range from 400-700 nm, where it is used for in-depth analysis of plant morphology, architecture, and extraction of color index features.

1. The imaging unit contains a rotating table for precise positioning of the tray and simultaneously allows multi-angle imaging for side views.
2. Set RGB imaging based on side-view imaging to capture the plant from three angles (0°, 120°, and 240°), which is taken in line scanning mode (RGB1) and top-view imaging in snapshot mode (RGB2).
3. Both cameras have an LED-based light source, ensuring homogeneous lighting of the imaged plant and, thus, accurately determining morphological and color features.
4. Extract calculated parameters by using data analyzer software.
5. For additional parameters based on side and top views, calculate the plant volume (digital biomass)[36]:

$$Volume_{plant} = \sqrt{Area_{side\ view}{}^2 \times Area_{top\ view}}$$

6. Calculate the relative growth rate (RGR)[37]:

$$RGR_{Tn+1} = \frac{ln(Volume_{Tn+1}) - ln(Volume_{Tn})}{(Tn+1 - Tn)}$$

Where T_n and T_{n+1} indicate the time interval (days).

4. Hyperspectral imaging

NOTE: Hyperspectral imaging is used for the visualization of the spectral reflectance of the plants. The changes in leaf reflectance are indicators of the different physiological status of the given plant.

1. Use the hyperspectral imaging sensor to quantify canopy reflectance in the visible part of the light spectra, with a visible-near-infrared (VNIR) hyperspectral camera in range 380-900 nm and a short-wavelength infrared camera (SWIR) in range 900-1700 nm.
2. The cameras are mounted on a robotic arm with an implemented halogen tube light source (600 W) for homogenous and spectrally appropriate sample illumination during image acquisition moving across the XZ area.
3. Both cameras operate in line scan mode and are placed in a light-insulated imaging box.
4. Before each measurement round, perform two calibration measurements (automatically): dark current calibration and radiometric calibration using the spectral reflectance Teflon standard.
5. The dark calibration image is subtracted from the raw and white calibration image to remove the dark current noise. Then, generate the final hyperspectral by dividing the raw image after subtraction by the white calibration image.

6. Exporting data and Image analysis

1. Use the data analyzer software for automatic extraction, background subtraction, and **Plant Mask** segmentation of the image processing pipeline (**Figure 2B**).
2. The software performs a fully automated analysis where mask application, background subtraction in which plants are isolated from their background, and parameter calculation are processed as described for RGB imaging[38] and thermal imaging[20].
3. Extract the measured and calculated parameters from the plant-specific pixels as defined by the RGB image-generated **Plant Mask** and **Tray Mask**.
4. If the images were not fully selected, which can occur due to changes in vegetation greenness during later developmental stages or the effect of stress treatment,

open the local data analysis part in the software and re-adjust **Plant Mask** settings in the data analyzer software dependent on each sensor.

5. In chlorophyll fluorescence image processing, adjust the chlorophyll fluorescence **Plant Mask** settings analysis parameters (**Supplementary Figure 4**).
    1. Set the threshold as **True**, meaning that plant segmentation is performed automatically.
    2. Set the **Mask Frame Index** as **False**, meaning that for **Plant Mask** detection, the Time-Visual frame is used as defined in chlorophyll fluorescence protocol.
6. In thermal image processing, set the parameters for the **Plant Mask** analysis (**Supplementary Figure 5**).
    1. Set the automatic threshold for the **Object Mask Generation** as **False**.
    2. Set the mask from **RGB side image** as **True** to be used for analysis.
7. In RGB image processing, adjust **Plant Mask** settings analysis parameters (**Supplementary Figure 6** and **Supplementary Figure 7**) depending on the species and the developmental stage.
    1. Select the formula **4*G-3*B-R**, which is the definition for object mask generation and defines the color component used (Red, Green, Blue component).
    NOTE: This standard formula and other settings can change depending on the type of camera used (Top or size view), applied treatment, and different cultivars.
    2. Adjust the **Threshold** used for conversion of the grayscale image with an enhanced green channel to a binary image-determining the surface covered by the plant.
    3. Adjust the **Median Filter Size** used to reduce the noise and invalid pixels and fill in missing ones.
    4. Adjust the **Minimal size of the object** in pixels to be included in the analysis.
    5. Adjust the **Minimal Size of holes** in the mask objects in pixels, typically tens of pixels. The holes smaller than this value are closed and taken into the object pixels.
    6. Set the **Use Reflection Reduction** as **True** for normalizing RGB values in each pixel.
    7. Set the **Skip Bad Exposed Points** as **True** for cropping over/under exposed pixels from the plant mask (e.g., omission of the surface reflections or the dark pixels where the noise is larger than the signal).
8. Color the segmentation settings analyzed from RGB using the data analyzer software to provide information about color changes related to stress responses and plant senescence.
    NOTE: Greenness is estimated using a pre-defined range of colors representing all stages of plant development. The intensity in color channels from all pixels corresponding to the plant surface was grouped and clustered to be used as a source color map for color segmentation.
    1. Provide the processed RGB image (removed background), color map - list of hues for specific analysis, as an input in the software.
    2. To get unbiased results, perform hues selection using a "training" dataset and select different developmental stages and treatments.
    NOTE: Analysis saves R, G, and B values of each pixel of each image from this training dataset.

3. Define the number of hues (select 6 hues) using the software for the color definition output, ranging from 0-255 for each channel.
4. Provide the list of hues generated in the data analyzer software (**Colors**).

9. In hyperspectral image processing, process the acquired hyperspectral data using the pixel-by-pixel analysis implemented in the hyperspectral analyzer software, featuring radiometric and dark noise calibration, background subtraction, and plant mask segmentation. Use the average spectra and vegetation indices for further analysis.
10. Create the mask for data extraction from the hyperspectral image from the VNIR image taken by the VNIR Hyperspectral camera. For the SWIR hyperspectral scan, generate a plant mask based on SWIR analysis.
    1. In **VNIR Plant Mask**, use the formula **1.2*(2.5*(R740-R672)-1.3*(R740-R556))** for visualizing the images where R represents reflectance value in a specific wavelength (**Supplementary Figure 8**).
    2. In **SWIR Plant Mask**, use the formula **(R960-R1450)-(R960-R1200)** in image processing for visualizing the images (**Supplementary Figure 9**).

7. Weighing and watering

1. Store the weight (before) watering during the weighing and watering procedure. Then apply watering, and keep the weight after watering as well.
2. Water the trays in the reference mode - each tray had a reference value stored in the database, to which it was always watered. Determine the reference based on the treatment.

8. Data analysis

1. Analyze the data using ANOVA and Shapiro test.
2. Conduct Pairwise comparisons between different treatments by Pairwise Wilcox test in R studio (version 4.2.3) using (dplyr), (tidyverse), (rstatix), and (ggpubr) packages.

   NOTE: The image analysis was automatically done by using data analyzer software. For further analysis of the image acquisition, use sensor-specific data analyzer software.

Representative Results

In this study, automated image-based phenotyping was used to investigate the morphological and physiological responses of potato (cv. Lady Rosetta) under single and combined stress. The applied approach showed the dynamic responses of plants in high spatio-temporal resolution when stress was induced at the tuber initiation stage. To assess the early and late phases of stress, the results were presented as 3 time periods ([0-5 days of phenotyping (DOP)], [6-10 DOP], and [11-15 DOP]) (**Figure 1**). Until 0 DOP, all plants were grown under control conditions (C), then from 1-5 DOP, where waterlogging stress (W) and heat stress (H) were applied. Thus, the responses were observed as follows: (i) in 0-5 DOP, indicated the initial heat and waterlogging; (ii) in 6-10 DOP, reflected the early drought (D) and combined heat and drought (HD) was observed and (iii) in 11-15 DOP, showed the late heat, drought and combined heat + drought + waterlogging (HDW) stresses. The recovery from waterlogging was observed in 6-10 DOP and 11-15 DOP.

Morphological traits

RGB imaging was applied to determine the effect of different stresses and combinations on above-ground plant growth. The results in **Figure 4** show that heat treatment and waterlogging stress (0-5 DOP) already cause a reduction of plant volume and RGR compared to control. During 6-10 DOP, plant volume and RGR of control plants continuously increased, while under heat, combined heat, drought, and waterlogging, this increase in plant volume was clearly reduced (**Figure 4A**). As plants are very susceptible to waterlogging stress, a decrease was pronounced in RGR (**Figure 4B**). During late drought stress (11-15 DOP), where SRWC was maintained at 20%, a clear reduction in RGR was observed compared to the control. However, in the late phase of combined HDW, the application of waterlogging treatment caused an increase in RGR on the last day of stress.

Physiological traits

The combination of structural and physiological phenotyping was applied to reveal further responses to stress. Using multiple imaging sensors enables the determination of the physiological responses under the early phase of stress. Further analysis of the chlorophyll fluorescence data showed that waterlogging was negatively affecting the photosynthetic efficiency where F_v'/F_m' (F_v/F_m_Lss) decreased dramatically in 0-5 DOP and 6-10 DOP, but a recovering response was observed in 11-15 DOP where F_v'/F_m' slightly increased (**Figure 5A**). During the late stress phase (11-15 DOP), a reduction of F_v'/F_m' was observed in drought and combined heat and drought. In waterlogged plants, the operating efficiency of plants (QY_Lss aka. φ_{PSII}) was significantly lower compared to other treatments in 0-5 DOP and 6-10 DOP but a slight increase at 11-15 DOP, thus indicating plant recovery (**Figure 5B**). Moreover, the different mechanisms in regulating the efficiency contributing to the protection of PSII were determined by calculating the fraction of open reaction centers in PSII in a light steady-state (qL_Lss) (**Figure 5C**). Only under drought was an increase in qL observed, probably due to photoinhibition.

These findings were in accordance with IR data that reflected different underlying mechanisms under stresses (**Figure 6**). An increase in deltaT (ΔT) was observed in waterlogging, reducing the gas exchange rate. Under late drought and combined heat and drought stresses, an increase in ΔT was due to stomata closure, considered one of the primary responses to avoid excess water loss. On the other hand, a reduction in ΔT under heat treatments was observed as stomata open to enhance the transpiration efficiency and cool the leaf surface.

By investigating the hyperspectral data, two parameters were selected from the hyperspectral VNIR data to assess the leaf reflectance indices, including NDVI as an indicator of chlorophyll content and PRI as an indicator of the efficiency of photosynthesis. The results showed a decrease in NDVI and PRI only under waterlogging in connection to the reduction observed in the morphological traits (**Figure 7A**,**B**). Furthermore, from the SWIR hyperspectral data used for assessing the water content in the plants, an increase in water index in waterlogging was observed during 0-5 DOP (**Figure 7C**). However, under heat treatments, an opposite response was observed where the water index was lower than the control. These findings were in accordance with an examination of vegetation from the color segmentation of RGB Top view. The changes in the proportion of hues indicate the stress responses over time (**Figure 8**). The greening index showed a reduction in the pigment content under drought and combined HDW at the late stress phase and gradual recovery from waterlogging treatment. Thus, using the multiple imaging sensors reflected the correlation

of morpho-physiological traits and enabled the assessment of the overall plant performance under abiotic stresses.

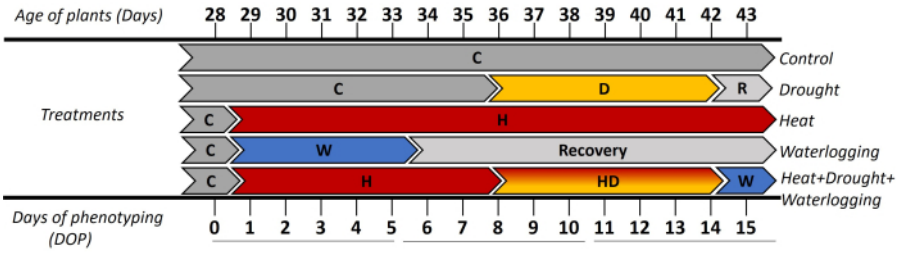

Figure 1: Timeline of applying the different treatments, including the age of plants in days after transplanting the *in vitro* cuttings. Day 0 of phenotyping (DOP) was measured under control (C) conditions, and then the different stresses were induced with different durations. From 1-5 DOP waterlogging (W) stress was applied and the initial response of heat treatment (H). The following days 6-10 DOP, where the initial phase of drought stress (D) and combined heat and drought stress (HD) were presented. During 11-15 DOP, the response of plants to the late phase of drought and heat treatments and the application of waterlogging to HD (HDW) for 1 day was reflected. Please click here to view a larger version of this figure.

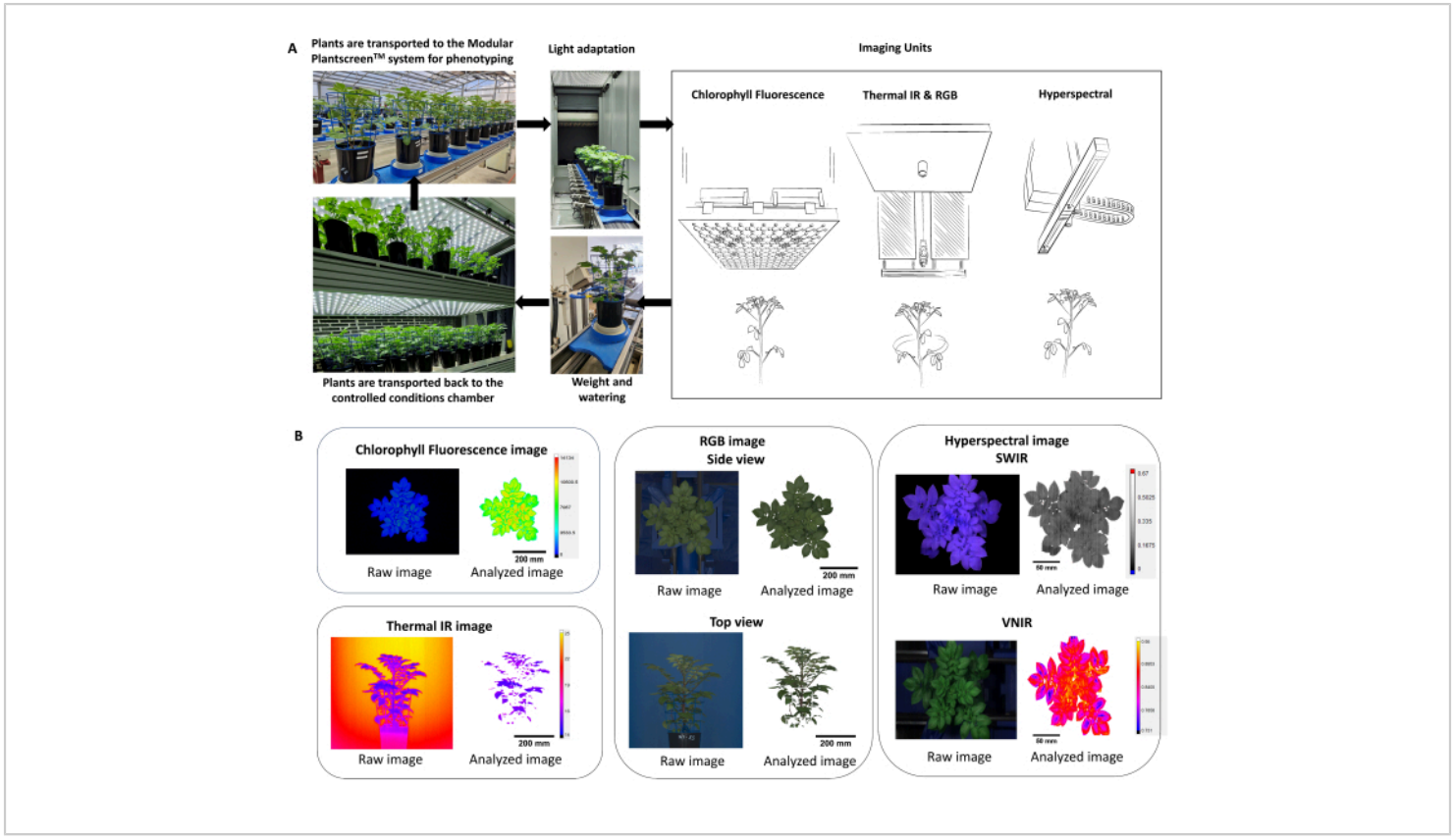

Figure 2: Scheme summarizing the phenotyping protocol and data analysis. (**A**) Overview of the phenotyping protocol. Plants are transported to the phenotyping system from the controlled conditions at the FS-WI growth chamber (PSI). Plants were light acclimated in the light adaptation chamber for 5 min at 500 µmol.m^{-2}.s^{-1} before the measurements. Multiple imaging sensors were used to determine morphological and physiological traits, followed by the weighting and watering station. Depending on the treatment, plants were placed back in controlled conditions, either at 22 °C/19 °C or 30 °C/28 °C. (**B**) Automatic extraction and segmentation of the image processing pipeline from each imaging sensor. Please click here to view a larger version of this figure.

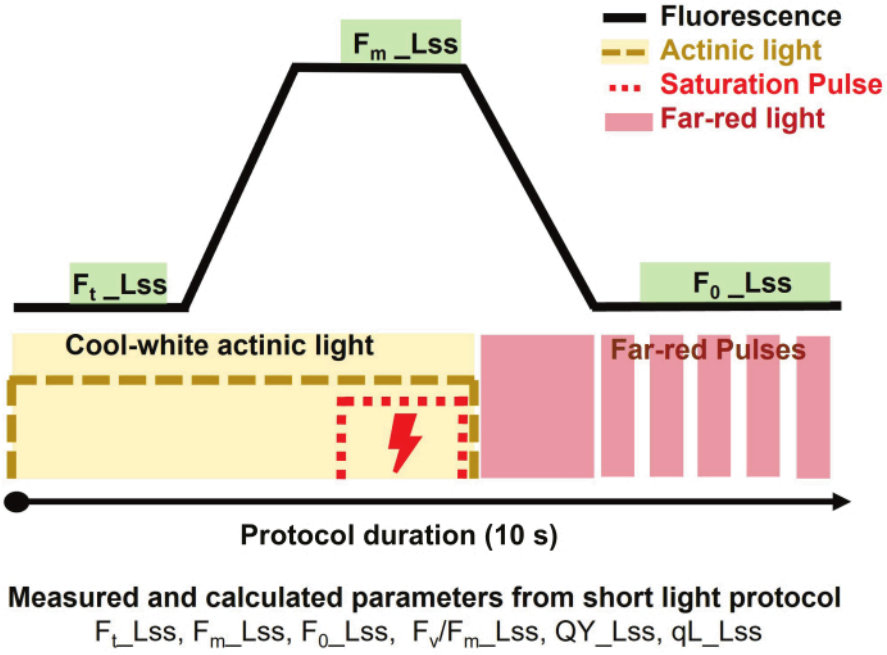

Figure 3: Short light protocol overview for chlorophyll fluorescence imaging. The measuring protocol started by turning on cool-white actinic light to measure the steady-state fluorescence in light (F_t_Lss) and then applying a saturation pulse to measure the steady-state maximum fluorescence in light (F_m_Lss). The actinic light was turned off, and the Far-red light was turned on to determine the steady-state minimum fluorescence in light (F_o_Lss). The duration of the protocol was 10 s per plant. Please click here to view a larger version of this figure.

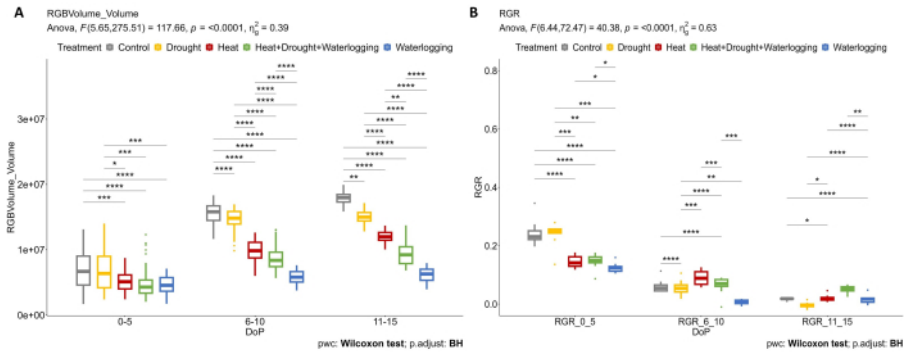

Figure 4: RGB imaging used for morphological assessment. (**A**) Plant volume calculated from the RGB top and side views area. (**B**) Relative growth rate (RGR) during the tuber initiation stage. The data represent mean values ± standard deviation (n = 10). Please click here to view a larger version of this figure.

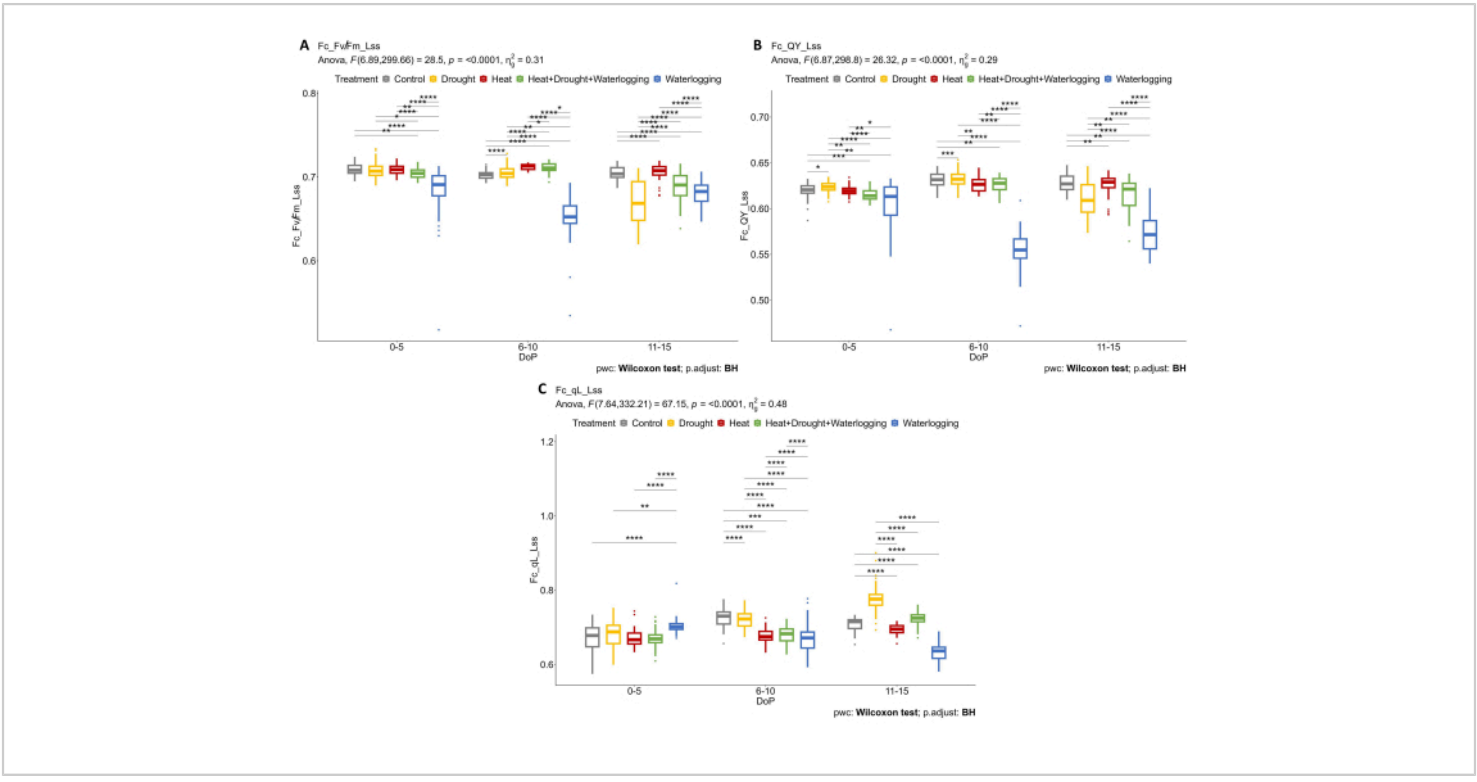

Figure 5: Chlorophyll fluorescence imaging on light-adapted plants. (**A**) Maximum efficiency of PSII photochemistry of light-adapted sample in light steady-state (F_v/F_m_Lss). (**B**) Photosystem II quantum yield or operating efficiency of photosystem II in light steady-state (QY_Lss). (**C**) Fraction of open reaction centers in PSII in light steady-state (oxidized QA) (qL_Lss). The data represent mean values ± standard deviation (n = 10). Please click here to view a larger version of this figure.

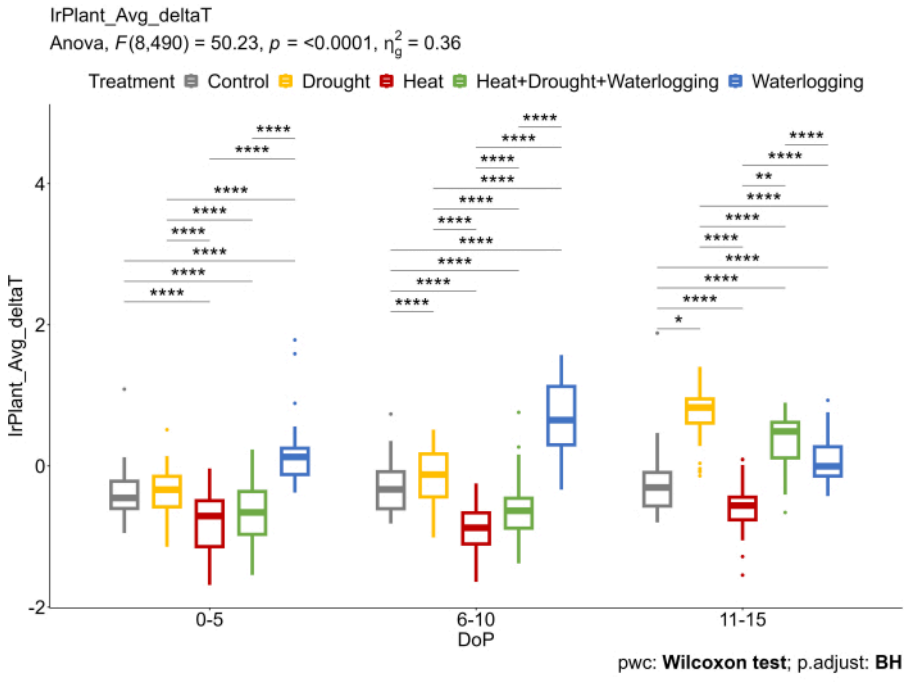

Figure 6: Thermal IR imaging was used to calculate the difference between canopy average temperature extracted from thermal IR images and air temperature (ΔT). The data represent mean values ± standard deviation (n = 10). Please click here to view a larger version of this figure.

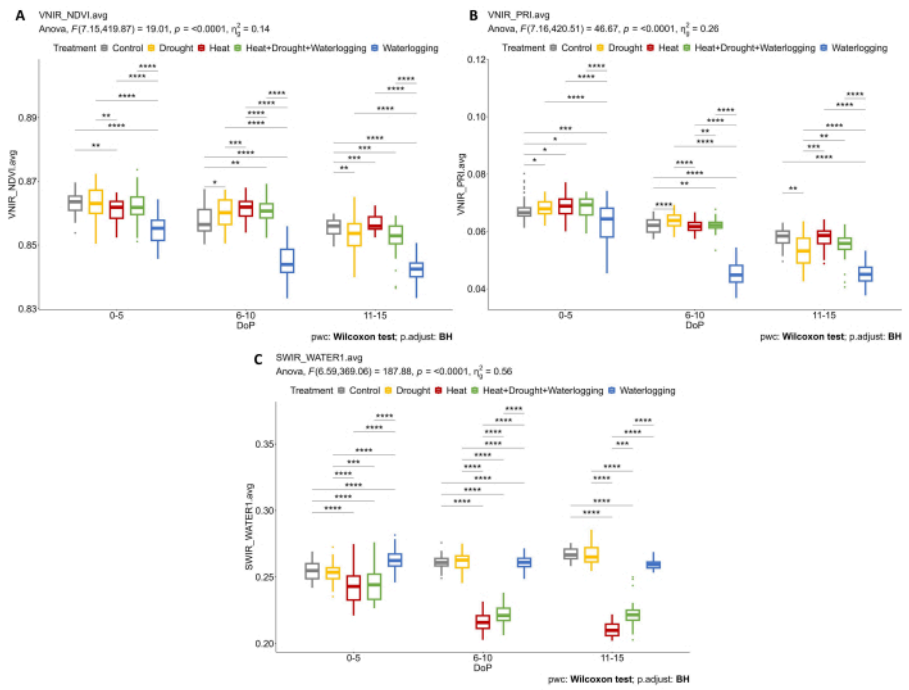

Figure 7: Hyperspectral imaging for determining vegetation indices and water content. (**A**) Normalized Difference Vegetation Index (NDVI). (**B**) Photochemical Reflectance Index (PRI) calculated from VNIR imaging. (**C**) Water index calculated from SWIR imaging. The data represent mean values ± standard deviation (n = 10). Please click here to view a larger version of this figure.

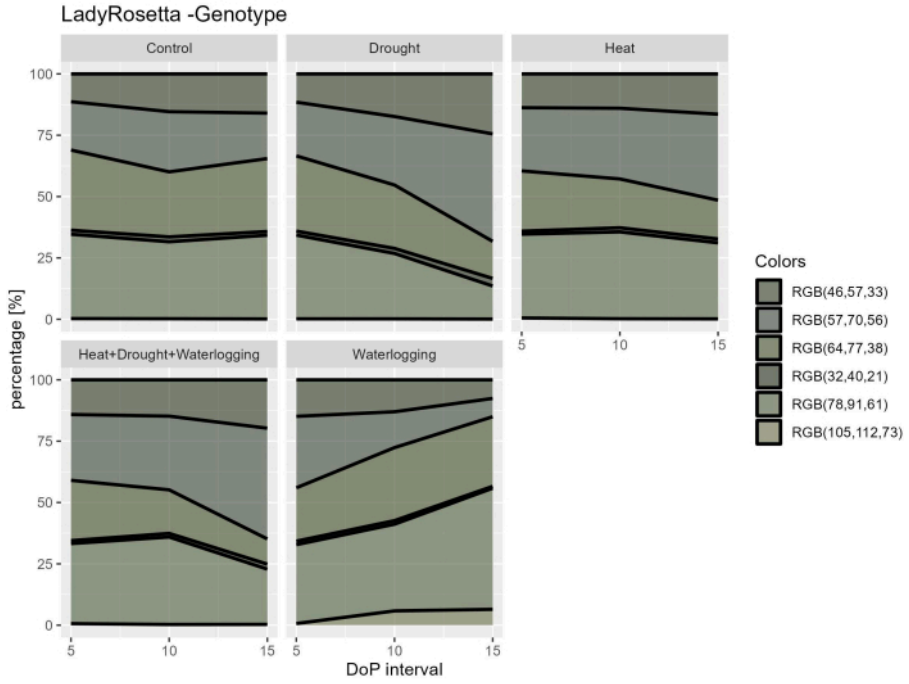

Figure 8: Greening index for plants under different treatments. Image processing is based on the transformation of the original RGB image in a color map consisting of 6 defined hues. The data represent mean values ± standard deviation (n = 10). Please click here to view a larger version of this figure.

Supplementary Figure 1: Light intensity measured during the days of phenotyping (DOP). The duration of measurements from 9:00 am to 12:35 pm. LI_Buff refers to the median data from 5 light sensors distributed in the greenhouse. Please click here to download this File.

Supplementary Figure 2: Relative humidity (RH) measured during the days of phenotyping (DOP). The duration of measurements from 9:00 am to 12:35 pm. RH_Buff refers to the median data from 5 humidity sensors distributed in the greenhouse. RH2 refers to the relative humidity in the adaptation chamber. Please click here to download this File.

Supplementary Figure 3: Temperature measured during the days of phenotyping (DOP). The duration of measurements from 9:00 am to 12:35 pm. T_Buff refers to the median data from 5 temperature sensors distributed in the greenhouse. T2 refers to the temperature in the adaptation chamber. T3 refers to the temperature of the heating wall. T4 refers to the temperature in the thermal IR imaging unit. Please click here to download this File.

Supplementary Figure 4: Screenshot from data analyzer software showing the parameters adjusted for plant mask analysis in chlorophyll fluorescence imaging sensors. Please click here to download this File.

Supplementary Figure 5: Screenshot from data analyzer software showing the parameters adjusted for plant mask analysis in thermal infrared imaging sensors. Please click here to download this File.

Supplementary Figure 6: Screenshot from data analyzer software showing the parameters adjusted for plant mask analysis in RGB 1-side view imaging sensors. Please click here to download this File.

Supplementary Figure 7: Screenshot from data analyzer software showing the parameters adjusted for plant mask analysis in RGB2-top view imaging sensors. Please click here to download this File.

Supplementary Figure 8: Screenshot from data analyzer software showing the parameters adjusted for plant mask analysis in VNIR imaging sensors. Please click here to download this File.

Supplementary Figure 9: Screenshot from data analyzer software showing the parameters adjusted for plant mask analysis in SWIR imaging sensors. Please click here to download this File.

Discussion

Improved advanced high-resolution imaging tools and computer vision techniques have enabled the rapid development of plant phenotyping to obtain quantitative data from massive plant images in a reproducible manner[39]. This study aimed to adapt and optimize high throughput image-based methodology using an array of currently available imaging sensors to monitor the dynamic responses of plants under single and combined abiotic stresses. A few critical steps of the applied approach require adjustments, including applying stress and selecting a suitable imaging protocol for the measurements. Using multiple sensors for image acquisition allows the quantification of key phenotypic traits (such as plant growth, photosynthetic efficiency, stomatal regulations, leaf reflectance, etc.). In addition, improves the understanding of how potato plants respond to different abiotic stresses. This is a key prerequisite for accelerating plant breeding projects to develop climate-tolerant genotypes[40]. The morphological responses to the induced stress depend on the development stage. For example, inducing stress at the stolon or tuber initiation stage inhibits leaf and plant development and limits the number of stolons, thereby reducing the final yield[41]. However, under unfavorable conditions, plants utilize stress responses as an adaptive response to prevent and repair stress-induced cellular damage[42]. Plants have adaptive mechanisms to avoid and tolerate stress conditions depending on the severity level[43].

To understand the mechanisms of plants, inducing the appropriate duration and intensity of stress and determining the plant responses to stress by using imaging sensors is considered one of the critical steps. When several stresses coincide, the intensity of one stress can overrule the effect of the others depending on the combination, intensity, and duration of the stresses. Thus, the stress effects can add up, or opposing responses can (partially) cancel each other, ultimately resulting in positive or negative effects on plants. The protocol selected in this study was based on previous experience to ensure that sufficient stress levels were applied. For instance, the application of the drought stress was adjusted to a moderate level as in a previous experiment, the response was not different from control treatments at an early stage of stress based on chlorophyll fluorescence imaging. This is due to the occurrence of photorespiration that acts as an alternative sink for electrons in the thylakoid membrane and a protective mechanism for the photosystem

II[44,45]. Under the combined stress response, plant exposure to a mild primary stressor could enhance tolerance to a following stressor, which can have a beneficial or detrimental impact[46]. In this study, a stronger response was observed under combined stress compared to individual drought stress. By investigating other physiological responses, the results showed an increase in ΔT (deltaT) under drought as stomata close to avoid excess water loss. In contrast, the reverse response was observed under heat stress where ΔT was lower compared to control reflecting stomata opening to enhance leaf cooling in accordance with the findings in wheat under combined heat and drought stress[20]. During waterlogging, the increase of ΔT due to stomatal closure resulted from oxygen deficiency in the soil and disruption of root water homeostasis, thereby lowering the transpiration stream with an increase in the ABA, a key hormone in water stress responses[47].

In plant stress studies, the duration of stress and subsequent recovery treatments is directly proportional to the stress intensity. For instance, moderate drought stress, such as maintaining soil moisture at 20% field capacity (FC), induces reversible phenotypic changes that typically recover after a single day of re-irrigation. In contrast, severe stress conditions like waterlogging result in extensive phenotypic damage, necessitating a longer recovery period. Although standardizing treatment durations is ideal, the inherent variability in stress intensities must be accounted for in experimental design.

The second critical step is to select an appropriate protocol and optimize the settings for each sensor. Chlorophyll fluorescence is a powerful tool in determining the performance of photosynthetic apparatus under stress[48]. Different chlorophyll fluorescence measuring protocols can be selected with either light or dark-adapted plants depending on the research question and the experimental design[49]. In this study, the selected protocol (short light response) enables the determination of various traits, including F_v'/F_m', φ_{PSII}, and qL, which indicate the photosynthesis performance under different conditions[50]. Previous studies showed that the used protocol in high-throughput phenotyping is effective in investigating the photosynthetic efficiency of plants under different applications of stress treatments and discriminating between healthy and stressed plants[14,20]. Based on the experimental design, it is very critical to consider the duration of the selected protocol when measuring in a high throughput system with a high plant population. Thus, the chlorophyll fluorescence measurement on light-adapted plants using a short-time protocol was selected to discriminate responses under different treatments. Genotype-environment interactions can influence many phenotypic traits, which is critical during measurement[12]. It is essential to consider that the duration of the measurement should be completed in a short time to minimize the diurnal effect on photosynthetic limitations[51].

Thermal IR imaging was used to determine the canopy temperature and understand the stomatal regulation under different treatments[52]. It is worth mentioning that technological optimization was used where the heating wall was located on the opposite side of the camera, and the wall's temperature was dynamically controlled and programmable. Thus, adjusting the background heated wall with integrated environmental sensors is necessary to properly select plants from the background by increasing the contrast of the background temperature over the temperature of the imaged object.

Even though image analysis is automated, adjusting RGB thresholding indexes is still required to obtain a proper binary mask in RGB imaging to precisely select plants[53]. In addition, choosing multiple angles is important for appropriately estimating quantitative parameters, including digital biomass and growth rate. In this study, three angles (0°, 120°, and 240°) on the RGB side view were selected and averaged to calculate the plant volume and relative growth rate accurately.

Depending on the spectral range, many physiological traits can be investigated using hyperspectral imaging[54]. It is necessary to determine which of the reflectance indices provides the necessary information and shows the response of plants under different conditions[14]. It is highly demanded in screening for tolerant varieties and plant phenotyping to determine the correlation between the hyperspectral indices and other physiological traits[55]. In this study, plants under waterlogging treatment showed a pronounced response in the chlorophyll content and photosynthetic efficiency from the VNIR imaging. Moreover, different responses were observed in the water index calculated from SWIR imaging under heat treatments and waterlogging due to different stomatal regulations and water content in the leaves.

Thus, these findings highlight the utility of such an approach after optimizing the settings and the potential of using multiple sensors to find stress traits relevant to climate tolerance. Assessing the dynamics of the responses using multiple imaging sensors can be used as one of the powerful tools in improving breeding programs.

Disclosures

The authors declare that they have no known competing financial interests or personal relationships that could have appeared to influence the work reported in this paper.

Acknowledgments

This ADAPT project (Accelerated Development of multiple-stress tolerant Potato) has received funding from the European Union's Horizon 2020 research and innovation program under grant agreement No GA 2020 862-858. This work was partially supported by the Ministry of Education, Youth and Sports of the Czech Republic with the European Regional Development Fund-Project "SINGING PLANT" (no. CZ.02.1.01/0.0/0.0/16_026/0008446). The Core Facility Plants Sciences of CEITEC MU is acknowledged for its cultivation facility support. We acknowledge Meijer BV for providing the in-vitro cuttings used in this study. We thank Lenka Sochurkova for assisting in the graphical design of Figure 2 and Pavla Homolová for helping with the preparation of plant material during the experiments at Photon Systems Instruments (PSI) Research Center (Drásov, Czech Republic).

References

1. IPCC. Climate Change 2021: The Physical Science Basis. *Contribution of Working Group I to the Sixth Assessment Report of the intergovernmental Panel on Climate change.* At <doi:https://www.ipcc.ch/report/ar6/wg1/> (2021).
2. Ray, D. K., Gerber, J. S., Macdonald, G. K., West, P. C. Climate variation explains a third of global crop yield variability. *Nat Commun.* **6**, 5989 (2015).
3. Acevedo, M. et al. A scoping review of adoption of climate-resilient crops by small-scale producers in low- and middle-income countries. *Nat Plants.* **6** (10), 1231-1241 (2020).

4. van Dijk, M., Morley, T., Rau, M. L., Saghai, Y. A meta-analysis of projected global food demand and population at risk of hunger for the period 2010-2050. *Nat Food.* **2** (7), 494-501 (2021).
5. Handayani, T., Gilani, S. A., Watanabe, K. N. Climatic changes and potatoes: How can we cope with the abiotic stresses? *Breed Sci.* **69** (4), 545-563 (2019).
6. Devaux, A., Goffart, J. P., Kromann, P., Andrade-Piedra, J., Polar, V., Hareau, G. The potato of the future: Opportunities and challenges in sustainable agri-food systems. *Potato Res.* **64** (4), 681-720 (2021).
7. Dahal, K., Li, X. Q., Tai, H., Creelman, A., Bizimungu, B. Improving potato stress tolerance and tuber yield under a climate change scenario - a current overview. *Front Plant Sci.* **10**, 563 (2019).
8. Ahmad, U., Sharma, L. A review of best management practices for potato crop using precision agricultural technologies. *Smart Agricultural Technology.* **4**, 100220 (2023).
9. Cabello, R., Monneveux, P., De Mendiburu, F., Bonierbale, M. Comparison of yield based drought tolerance indices in improved varieties, genetic stocks and landraces of potato (Solanum tuberosum L.). *Euphytica.* **193** (2), 147-156 (2013).
10. von Gehren, P. et al. Farmers feel the climate change: Variety choice as an adaptation strategy of European potato farmers. *Climate.* **11** (9), 189 (2023).
11. Fiorani, F., Schurr, U. Future scenarios for plant phenotyping. *Annu Rev Plant Biol.* **64**, 267-291 (2013).
12. Poorter, H. et al. Pitfalls and potential of high-throughput plant phenotyping platforms. *Front Plant Sci.* **14**, 1233794 (2023).
13. Berger, B., de Regt, B., Tester, M. High-throughput phenotyping of plant shoots. *Methods Mol Biol.* **918**, 9-20 (2012).
14. Humplík, J. F., Lazár, D., Husičková, A., Spíchal, L. Automated phenotyping of plant shoots using imaging methods for analysis of plant stress responses - a review. *Plant Methods.* **11**, 29 (2015).
15. Danilevicz, M. F., Bayer, P. E., Nestor, B. J., Bennamoun, M., Edwards, D. Resources for image-based high-throughput phenotyping in crops and data sharing challenges. *Plant Physiol.* **187** (2), 699-715 (2021).
16. Abebe, A. M., Kim, Y., Kim, J., Kim, S. L., Baek, J. Image-based high-throughput phenotyping in horticultural crops. *Plants.* **12** (10), 2061 (2023).
17. Lazarević, B., Carović-Stanko, K., Safner, T., Poljak, M. Study of high-temperature-induced morphological and physiological changes in potato using nondestructive plant phenotyping. *Plants.* **11** (24), 3534 (2022).
18. Marchetti, C. F. et al. A novel image-based screening method to study water-deficit response and recovery of barley populations using canopy dynamics phenotyping and simple metabolite profiling. *Front Plant Sci.* **10**, 1252 (2019).
19. Kim, S. L. et al. High-throughput phenotyping platform for analyzing drought tolerance in rice. *Planta.* **252** (3), 38 (2020).
20. Abdelhakim, L. O. A., Rosenqvist, E., Wollenweber, B., Spyroglou, I., Ottosen, C. O., Panzarová, K. Investigating combined drought- and heat stress effects in wheat under controlled conditions by dynamic image-based phenotyping. *Agronomy.* **11** (2), 364 (2021).

21. Zandalinas, S. I., Sengupta, S., Fritschi, F. B., Azad, R. K., Nechushtai, R., Mittler, R. The impact of multifactorial stress combination on plant growth and survival. *New Phytologist.* **230** (3), 1034-1048 (2021).
22. Raza, A. et al. Impact of climate change on crops adaptation and strategies to tackle its outcome: A review. *Plants.* **8** (2), 34 (2019).
23. Nasir, M. W., Toth, Z. Effect of drought stress on potato production: A review. *Agronomy.* **12** (3), 635 (2022).
24. Wagg, C., Hann, S., Kupriyanovich, Y., Li, S. Timing of short period water stress determines potato plant growth, yield and tuber quality. *Agric Water Manag.* **247**, 106731 (2021).
25. Yamauchi, T., Colmer, T. D., Pedersen, O., Nakazono. M. Regulation of root traits for internal aeration and tolerance to soil waterlogging-flooding stress. *Plant Physiol.* **176** (2), 1118-1130 (2018).
26. Aien, A., Chaturvedi,. A. K., Bahuguna, R. N., Pal, M. Phenological sensitivity to high temperature stress determines dry matter partitioning and yield in potato. *Indian J Plant Physiol.* **22** (1), 63-69 (2017).
27. Zandalinas, S. I., Mittler, R., Balfagón, D., Arbona, V., Gómez-Cadenas, A. Plant adaptations to the combination of drought and high temperatures. *Physiol Plant.* **162** (1), 2-12 (2018).
28. Suzuki, N., Rivero, R. M., Shulaev, V., Blumwald, E., Mittler, R. Abiotic and biotic stress combinations. *New Phytologist.* 203 (1), 32-43 (2014).
29. Atkinson, N. J., Jain, R., Urwin, P. E. *The Response of Plants to Simultaneous Biotic and Abiotic Stress.* In *Combined Stresses in Plants.* Springer, Cham (2015).
30. Harris, P. M. *The Potato Crop.* 2nd ed. (Harris PM, ed.). Springer, Dordrecht (1992).
31. Weisz, R., Kaminski, J., Smilowitz, Z. Water deficit effects on potato leaf growth and transpiration: Utilizing fraction extractable soil water for comparison with other crops. *Am Potato J.* **71** (12), 829-840 (1994).
32. Wang, X., Vignjevic, M., Jiang, D., Jacobsen, S., Wollenweber, B. Improved tolerance to drought stress after anthesis due to priming before anthesis in wheat (Triticum aestivum L.) var. Vinjett. *J Exp Bot.* **65** (22), 6441-6456 (2014).
33. Junker, A. et al. Optimizing experimental procedures for quantitative evaluation of crop plant performance in high throughput phenotyping systems. *Front Plant Sci.* **5**, 770 (2015).
34. Smith, S. M. et al. Diurnal changes in the transcriptome encoding enzymes of starch metabolism provide evidence for both transcriptional and posttranscriptional regulation of starch metabolism in arabidopsis leaves. *Plant Physiol.* **136** (1), 2687-2699 (2004).
35. Findurová, H., Veselá, B., Panzarová, K., Pytela, J., Trtílek, M., Klem, K. Phenotyping drought tolerance and yield performance of barley using a combination of imaging methods. *Environ Exp Bot.* **209**, 105314 (2023).
36. Klukas, C., Chen, D., Pape, J. M. Integrated analysis platform: an open-source information system for high-throughput plant phenotyping. *Plant Physiol.* **165** (2), 506-518 (2014).
37. Paul, K. et al. Understanding the biostimulant action of vegetal-derived protein hydrolysates by high-throughput plant phenotyping and metabolomics: A case study on tomato. *Front Plant Sci.* **10**, 47 (2019).

38. Awlia, M. et al. High-throughput non-destructive phenotyping of traits that contribute to salinity tolerance in Arabidopsis thaliana. *Front Plant Sci.* **7**, 1414 (2016).
39. Li, Z., Guo, R., Li, M., Chen, Y., Li, G. A review of computer vision technologies for plant phenotyping. *Comput Electron Agric.* **176**, 105672 (2020).
40. Li, L., Zhang, Q., Huang, D. A review of imaging techniques for plant phenotyping. *Sensors (Switzerland).* **14** (11), 20078-20111 (2014).
41. Obidiegwu, J. E., Bryan, G. J., Jones, H. G., Prashar, A. Coping with drought: Stress and adaptive responses in potato and perspectives for improvement. *Front Plant Sci.* **6**, 542 (2015).
42. Zhang, H., Zhao, Y., Zhu, J. K. Thriving under stress: How plants balance growth and the stress response. *Dev Cell.* **55** (5), 529-543 (2020).
43. Bandurska, H. Drought stress responses: Coping strategy and resistance. *Plants.* **11** (7), 922 (2022).
44. Wingler, A., Lea, P. J., Quick, W. P., Leegood, R. C. Photorespiration: metabolic pathways and their role in stress protection. *Philos Trans R Soc Lond B Biol Sci.* **355** (1402), 1517-1529 (2000).
45. Baker, N. R., Rosenqvist, E. Applications of chlorophyll fluorescence can improve crop production strategies: an examination of future possibilities. *J Exp Bot.* **55** (403), 1607-1621 (2004).
46. Georgieva, M., Vassileva, V. Stress management in plants: Examining Provisional and Unique Dose-Dependent Responses. *Int J Mol Sci.* **24** (6), 5105 (2023).
47. Leeggangers, H. A. C. F., Rodriguez-Granados, N. Y., Macias-Honti, M. G., Sasidharan, R. A helping hand when drowning: The versatile role of ethylene in root flooding resilience. *Environ Exp Bot.* **213**, 105422 (2023).
48. Baker, N. R. Chlorophyll fluorescence: a probe of photosynthesis in vivo. *Annu Rev Plant Biol.* **59** (1), 89-113 (2008).
49. Murchie, E. H., Lawson, T. Chlorophyll fluorescence analysis: a guide to good practice and understanding some new applications. *J Exp Bot.* **64** (13), 3983-3998 (2013).
50. Maxwell, K., Johnson, G. N. Chlorophyll fluorescence-a practical guide. *J Exp Bot.* **51** (345), 659-668 (2000).
51. Yokoyama, G., Ono, S., Yasutake, D., Hidaka, K., Hirota, T. Diurnal changes in the stomatal, mesophyll, and biochemical limitations of photosynthesis in well-watered greenhouse-grown strawberries. *Photosynthetica.* **61** (1), 1-12 (2023).
52. Jones, H. G. Application of thermal imaging and infrared sensing in plant physiology and ecophysiology. *Advances in Botanical Research.* **41**, 107-163 (2004).
53. Brainard, S. H., Bustamante, J. A., Dawson, J. C., Spalding, E. P., Goldman, I. L. A digital image-based phenotyping platform for analyzing root shape attributes in carrot. *Front Plant Sci.* **12**, 690031 (2021).
54. Huber, S., Tagesson, T., Fensholt, R. An automated field spectrometer system for studying VIS, NIR and SWIR anisotropy for semi-arid savanna. *Remote Sens Environ.* **152**, 547-556 (2014).
55. Mertens, S. et al. Proximal hyperspectral imaging detects diurnal and drought-induced changes in maize physiology. *Front Plant Sci.* **12**, 640914 (2021).